AIAA JOURNAL
Vol. 54, No. 12, December 2016

Model Reduction and Sensor Placement Methods for Finite Element Model Correlation

J. F. Mercer* and G. S. Aglietti†
University of Surrey, Guildford, England GU2 7XH, United Kingdom
and
A. M. Kiley‡
Airbus Defence and Space, Stevenage, England SG1 2AS, United Kingdom

DOI: 10.2514/1.J054976

The issue of model reduction is one that must often be overcome in order to perform the necessary checks as part of the spacecraft finite element model validation process. This work compares different reduction methods: specifically, the popular and longstanding Guyan method and the potentially more accurate system equivalent reduction expansion process. The influence of sensor set location on the quality of the reduced model is also considered, and the commonly applied methods to maximize kinetic energy and effective independence are applied. These investigations take the form of studies involving two large, unique, scientific spacecraft. The computational results are compared with experimental results that are also detailed in the paper. The findings highlight the potential issues with the accuracy of a Guyan reduced model in replicating the full system dynamics, even with a reasonably large sensor set. It is shown that this can be improved slightly in some circumstances through implementation of sensor set placement optimization techniques. The system equivalent reduction expansion process method is shown to have the benefit of being more accurate at replicating the full system behavior than the more traditional Guyan method while also producing higher diagonal values in cross-orthogonality comparisons between the finite element model and the test.

Nomenclature

a	=	candidate sensor set
$\boldsymbol{C}$	=	damping matrix
$\boldsymbol{f}$	=	applied force vector
$\boldsymbol{I}$	=	identity matrix
$\boldsymbol{K}$	=	stiffness matrix
$\boldsymbol{M}$	=	mass matrix
m	=	master degrees of freedom (to be retained)
$\boldsymbol{Q}$	=	Fisher independence matrix
s	=	slave degrees of freedom (to be eliminated)
$\boldsymbol{u}$	=	physical displacement
$\boldsymbol{\eta}$	=	modal displacement vector
$\boldsymbol{\Phi}$	=	modal matrix
$\boldsymbol{\phi}$	=	analytical mode shape vector
$\boldsymbol{\psi}$	=	experimental mode shape vector

I. Introduction

FROM a structural perspective, launch is one of the most challenging phases in the mission of a spacecraft. The interaction between the spacecraft and the launch vehicle is an important aspect of this; however, it is not possible to practically test the two systems coupled together. Thus, in order to simulate the launch environment, coupled loads analyses (CLAs) are carried out that couple a finite element model (FEM) of the spacecraft with one of the launcher to virtually predict flight loads. If there is to be confidence in the results of the CLA, it is necessary to first validate the spacecraft FEM against appropriate test-measured data in order to ensure that the math model is able to reproduce accurately the behavior of the physical hardware. A correlation process is therefore initiated, in which the analytical and experimental results are compared and the FEM updated to reconcile differences between test and analysis.

Comparisons between the test and finite element analysis (FEA) are made by using modal vector-based metrics, such as modal assurance criteria (MAC) [1] and cross-orthogonality checks (COCs) [2], where the MAC check is a comparison between two vectors (typically, the test-derived mode shapes and FEA eigenvectors) and the COC is an orthogonality check that uses the system mass matrix [3]. The use of the mass matrix serves to weight the degree-of-freedom (DOF) importance based on modal mass, which is not accounted for by the basic MAC check.

The use of the orthogonality metric does, however, introduce the issue of the order of the mass matrix. When computing the MAC, vectors describing the mode shapes must be of equal length. The FEM is likely to have data for hundreds of thousands, if not millions, of DOFs, compared to data for only a few hundred DOFs captured by accelerometers during the test. The MAC can nonetheless be used by simply partitioning out the FEM eigenvector values for DOFs corresponding to the test measurement point plan (MPP), and therefore does not require further manipulation of the model. For the orthogonality checks, the mass matrix dimensions must match the modal vector order. It is therefore necessary to either expand the experimental data to a DOF count matching the FEM or reduce the analytical results to the DOFs corresponding to the test accelerometers [4]. A potential problem with using the FEM to expand the test data is that any errors in the FEM, which is still to be validated, may corrupt the experimental data and undermine the following correlation and update process. It is therefore generally considered that the modal reduction of the FEM to the test measured DOFs, to create a test-analysis model (TAM) of the structure, is the preferred approach [5].

There are many methods currently available for performing these reductions. There have already been several studies [6–12] comparing the various methods, including static (or Guyan) reduction [13], the improved reduction system (IRS) [14], dynamic reduction [15], modal reduction [5], the system equivalent reduction expansion process (SEREP) [16], hybrid [17], and Craig–Bampton [18]. Here, the focus is on the Guyan reduction method, which has some historical basis and availability within finite element (FE) tools such as MSC Nastran [19]; and SEREP, which has been identified as potentially more suitable for generating spacecraft TAMs [20,21]. Where most previous work has focused on small, generic example

Received 22 January 2016; revision received 3 May 2016; accepted for publication 7 June 2016; published online 23 August 2016.

*Research Student, Surrey Space Centre.
†Professor, Surrey Space Centre.
‡Senior Specialist.

cases, the main contribution of this work is to show and identify how these methodologies perform with real spacecraft and typical FEMs generated in industry. Another aspect to be considered by this work is the influence of different sensor placement options on the respective reduction methods.

The choice of test sensor/accelerometer set location MPP is crucial in order to sufficiently capture the dynamics of the system. Good quality test data are vital if the resulting spacecraft FEM validation is to be meaningful. The experimental modal parameters used in the validation of spacecraft FEMs are typically estimated from data collected during fixed-base sine-sweep testing performed through use of an electrodynamic shaker. In specifying the MPP in preparation for a spacecraft sine test, usually, the first point of focus is capturing the response measurements at all unit or equipment mounting locations, key subsystem locations (often prescribed as suitable monitor locations by subsystem contractors), and CLA recovery locations. Such a primary focus on data recovery, in terms of obtaining inputs into the payload or responses on the payload, often accounts for a substantial portion of available channel count, which can leave a potential smaller subset available for which the purpose is primarily to support modal correlation. All modes of significance, both to the global structure and to any critical local modes on subsystems, must be captured with sufficient signal strength and have independence such that each mode is distinct and easily identified and differentiated from the other modes of the system. In addition, the spacecraft FEM correlation process requires the production of a good quality reduced TAM to increase the likelihood of achieving acceptable results for the COC. The quality of the final TAM depends heavily on the reduction method being employed and on the retained DOFs of the system. As such, pretest methods to improve the placement of sensors have been created [22–26].

Over the years, various sensor placement optimization methods have been developed that employ the FEM to identify a MPP set pretest, such that the data collected are of high quality for clear mode identification and for production of accurate, robust TAMs. Most methods involve the identification of the "best" degrees of freedom to keep from an initial larger candidate set; however, more recently, some methods have been developed that expand out from a small initial set to a larger final set [27]. Both iterative methods, such as the effective independence (EFI) method [28], and single calculation methods, such as modal kinetic energy (KE) [29], are available. Sensors may be considered individually as separate DOFs or in grouped form, such as in the case of triaxial sensors [30].

Flanigan [10] observed that certain reduction methods appeared to be more influenced than others by an inadequate sensor set. Bergman et al. [6] also explored different reduction methods, and they proposed that many previous studies, such as those by Chung and Simonian [8], Freed and Flanigan [9], and Avitabile et al. [11], had failed to account for the fact that different reduction methods required different sensor placement optimization methods. Most previous work exploring reduction methods had taken a single sensor set, determined from a particular sensor placement optimization method, and had compared the reduction methods for that particular set. As such, Bergman et al. [6] attempted to compensate for this by applying different sensor placement methods as appropriate for each reduction method, in order to assess the quality and robustness of the resulting TAMs with respect to the same original full FEM. Of the sensor placement methods considered, SEREP performed best when EFI [27] was applied to ensure optimum linear independence of target modes; whereas for static reductions, a KE-based technique was employed. It is therefore clear that the sensor placement method must be consistent with the reduction method to be employed, as the two are interconnected. As such, this work takes a similar approach, in that both EFI- and KE-based sensor placement techniques are explored. In addition to these optimized sensor placements, as considered in the works previously cited, this work also considers the real MPPs used in spacecraft testing, which account for practical considerations of accessibility and areas of interest to predict load levels around delicate equipment. Where the Bergman et al. study [6] focused on one simple, generic satellite FEM with fewer than 10,000 DOFs in total, this work considers two real, large, scientific spacecraft (BepiColombo and Aeolus) FEMs with complex architectures and DOF counts on the order of hundreds of thousands. The use of real spacecraft in this study has enabled final comparisons to be made between the FEM and the test mode shapes. Although previous work has investigated the robustness of reduction methods in theory using analytical models [21], the differences between test and FEM mode shapes can be caused by a wide variety of factors and, as such, can be difficult to replicate using purely mathematical analyses. In real testing, it is possible that not all vibration modes will be properly excited; the dynamic influence of coupling with the shaker structure can influence the responses; and there can be additional uncertainty in the test mode shapes introduced through curve-fitting estimations. The FEMs, which are often large and intricate, may not match the test due to a variety of issues; including "incorrect" modelling assumptions in regions which are difficult to represent, such as the rigid constraints applied at the base. The comparison with test data presented here allows for a realistic assessment of the suitability of the reduction methods to create reduced TAMs for an actual test–FEM correlation rather than more "academic" studies, the conditions of which often minimize or omit many of these factors. The fact that two real spacecraft have been considered gives wider relevance to the results of this work.

The studies presented herein are focused on the issues associated with the placement of accelerometers during modal testing and the subsequent reduction of the mathematical model to the corresponding DOFs. The need to perform such activities is a direct consequence of the use of discrete measurement methods (i.e., only having data at a limited number of selected discrete points on the test structure for comparison with the mathematical model). Many of the most established model reduction methods have been around for decades [31]. During that time, the number of accelerometers used on typical modal vibration tests has not increased in line with the increase in FEM "size," with FEMs comprising over a million DOFs now common in many applications (such as those considered in this paper). This increased mismatch in the amount of data from the test and FEM has exacerbated the issues associated with model reduction; as such, this work presents the results of reductions performed on larger, more complex FEMs than many of those considered in older studies or those focused on smaller/simpler academic example cases.

Full-field measurement methods and those able to capture data at more numerous points have been developed that may address some of the issues associated with the traditional discrete measurement techniques. These include the application of noncontact approaches, such as digital image correlation (DIC) [32,33] and the use of laser Doppler vibrometers (LDVs) [34,35]. The noncontact measurements will have the additional benefit of not mass loading the structure, which can be an issue with traditional methods employing sensors attached to the structure. The availability of full-field data may also enhance the ability to identify and distinguish subtleties in different vibration mode shapes from the test in cases where this may not have been achieved with a discrete MPP. Of the aforementioned optical measurement techniques, the use of LDVs is more common for vibration testing at present; however, issues including the expense and time required have so far limited the range of applications [31]. The development of experimental modal analysis methods employing DIC in three dimensions has shown feasibility, but the technology remains too immature [31] to be considered for industrial applications such as those addressed herein. Research into this subject is ongoing, with several studies comparing the more traditional modal testing methods (such as roving hammer tests using accelerometers) with these noncontact optical approaches [31,36], as well as work being undertaken to develop the new data processing and correlation methods necessary to account for large amounts of data gathered from the full field of interest [37–39].

Additionally, the field of strain modal analysis may become more widespread in years to come. The use of distributed fiber-optic strain sensors has become common in structural health monitoring [40]; however, their use may be broadened into modal testing applications as developments, such as fiber Bragg grating sensors [41], continue overcome some of the issues that had previously

inhibited the practicality of strain gauges versus the more easily applied accelerometers [42].

It is possible that the future of modal testing will lie in the use of the aforementioned methods. If full-field techniques become viable for large, complex structures, this may circumvent many of the issues concerning sensor placement and model reductions that are presented herein. Until such time as the cost and practicality issues associated with the full-field approaches are resolved, there is still value in pursuing the best sensor placement and model reduction methods for current discrete measurement applications.

II. Theory

A. Modal Correlation Checks

The MAC are a simple means to determine the level of similarity between two vectors of equal order. Typically in FEM correlations, the test mode shapes and FEM eigenvectors are compared, and the MAC check yields a value between zero and one that indicates how closely matched the vectors are, with one indicating a perfect match:

$$\mathrm{MAC} = \frac{(\boldsymbol{\psi}^T\boldsymbol{\phi})^2}{(\boldsymbol{\psi}^T\boldsymbol{\psi})\cdot(\boldsymbol{\phi}^T\boldsymbol{\phi})} \tag{1}$$

The experimental and analytical mode shapes are given here by $\boldsymbol{\psi}$ and $\boldsymbol{\phi}$, respectively.

It is generally considered, and indicated in the European Cooperation for Space Standardization (ECSS) standards [43] and similar NASA guidelines [44], that target modes achieving a MAC of at least 0.9 indicates a good correlation, and as such this is the target value for the fundamental modes of a spacecraft.

The COC is also an ECSS [43] required check and works similarly to MAC, but with the mass matrix employed to weight the relative importance of the DOFs being considered. An ideal result of perfectly matched mode shapes that are orthogonal to the mass matrix will yield a diagonal matrix and, for mass normalized modes, this becomes an identity matrix. In the ESA and NASA standards [43,44], it is specified that offdiagonal values less than 0.1 and leading diagonal terms greater than 0.9 are deemed to indicate a good level of correlation. The typical and normalized cross-orthogonality (NCO) forms of the COC are given by

$$\mathrm{COC} = \frac{(\boldsymbol{\psi}^T\boldsymbol{M}_{\mathrm{TAM}}\boldsymbol{\phi})}{\sqrt{(\boldsymbol{\psi}^T\boldsymbol{M}_{\mathrm{TAM}}\boldsymbol{\psi})}\sqrt{(\boldsymbol{\phi}^T\boldsymbol{M}_{\mathrm{TAM}}\boldsymbol{\phi})}} \tag{2}$$

$$\mathrm{NCO} = \frac{(\boldsymbol{\psi}^T\boldsymbol{M}_{\mathrm{TAM}}\boldsymbol{\phi})^2}{(\boldsymbol{\psi}^T\boldsymbol{M}_{\mathrm{TAM}}\boldsymbol{\psi})(\boldsymbol{\phi}^T\boldsymbol{M}_{\mathrm{TAM}}\boldsymbol{\phi})} \tag{3}$$

where the TAM, or reduced mass matrix $\boldsymbol{M}_{\mathrm{TAM}}$, is generated by application of an appropriate model reduction method. The experimental and analytical mode shapes are again given by $\boldsymbol{\psi}$ and $\boldsymbol{\phi}$, respectively.

B. Model Reduction Methods

1. Guyan Reduction

Guyan reduction has been considered for investigation, as it is one of the most commonly used reduction methods in industry. Due to its popularity, this reduction method is supported by many widely used FEA software packages; for example, this work has employed tools available through MSC Nastran software [19] to perform the reductions on the spacecraft FEMs.

Guyan reduction is a static reduction method, and therefore is not able to accurately capture the exact dynamics of the full system. Flanigan [10] showed that Guyan reduction produced a TAM that did not represent the full system as accurately as more sophisticated methods, such as the IRS and dynamic reduction, which had been developed subsequently to overcome the shortcomings of static methods. One reason for its continued popularity, despite its limitations, is that Guyan reduction is simple to perform and is incorporated through a production routine within certain FE codes. Another key advantage is that the resulting TAM also has been shown (e.g., by Chung and Simonian [8]) to have the benefit of being relatively robust, when compared to modal methods such as the SEREP, at achieving low offdiagonal COC results in spite of noise and small errors in the test or FEM.

The dynamics of a system can be defined by the following equation:

$$\boldsymbol{M}\ddot{\boldsymbol{u}} + \boldsymbol{C}\dot{\boldsymbol{u}} + \boldsymbol{K}\boldsymbol{u} = \boldsymbol{f} \tag{4}$$

where $\boldsymbol{M}$, $\boldsymbol{C}$, and $\boldsymbol{K}$ are the mass, damping, and stiffness matrices, respectively; $\boldsymbol{u}$ is the physical displacements; and $\boldsymbol{f}$ is the applied forces.

To perform the Guyan, or static, reduction, Eq. (4) can be written in the following partitioned form with the damping neglected:

$$\begin{bmatrix} \boldsymbol{M}_{\mathrm{mm}} & \boldsymbol{M}_{\mathrm{ms}} \\ \boldsymbol{M}_{\mathrm{sm}} & \boldsymbol{M}_{\mathrm{ss}} \end{bmatrix} \cdot \begin{Bmatrix} \ddot{\boldsymbol{u}}_m \\ \ddot{\boldsymbol{u}}_s \end{Bmatrix} + \begin{bmatrix} \boldsymbol{K}_{\mathrm{mm}} & \boldsymbol{K}_{\mathrm{ms}} \\ \boldsymbol{K}_{\mathrm{sm}} & \boldsymbol{K}_{\mathrm{ss}} \end{bmatrix} \cdot \begin{Bmatrix} \boldsymbol{u}_m \\ \boldsymbol{u}_s \end{Bmatrix} = \begin{Bmatrix} \boldsymbol{f}_m \\ 0 \end{Bmatrix} \tag{5}$$

Here, the subscripts m and s are used for the master and slave DOFs, respectively, where the masters are the DOFs of interest to be retained and the slaves are those to be eliminated in the reduction. In a Nastran context, the "masters" may be considered the problem A-set definition in Nastran terminology.

For the static reduction, the inertias of the slave DOFs are assumed small, and thus are neglected, allowing the second line of Eq. (5) to be simplified to

$$\boldsymbol{K}_{\mathrm{sm}}\boldsymbol{u}_m + \boldsymbol{K}_{\mathrm{ss}}\boldsymbol{u}_s \approx 0 \tag{6}$$

This allows for the slave displacements to be defined in terms of the master displacements, and this transformation may then be substituted back into Eq. (5) as follows:

$$\begin{bmatrix} \boldsymbol{M}_{\mathrm{mm}} & \boldsymbol{M}_{\mathrm{ms}} \\ \boldsymbol{M}_{\mathrm{sm}} & \boldsymbol{M}_{\mathrm{ss}} \end{bmatrix} \begin{bmatrix} \boldsymbol{I} \\ -\boldsymbol{K}_{\mathrm{ss}}^{-1}\boldsymbol{K}_{\mathrm{sm}} \end{bmatrix} \cdot \{\ddot{\boldsymbol{u}}_m\} + \begin{bmatrix} \boldsymbol{K}_{\mathrm{mm}} & \boldsymbol{K}_{\mathrm{ms}} \\ \boldsymbol{K}_{\mathrm{sm}} & \boldsymbol{K}_{\mathrm{ss}} \end{bmatrix} \begin{bmatrix} \boldsymbol{I} \\ -\boldsymbol{K}_{\mathrm{ss}}^{-1}\boldsymbol{K}_{\mathrm{sm}} \end{bmatrix} \cdot \{\boldsymbol{u}_m\} \approx \{\boldsymbol{f}_m\} \tag{7}$$

The slave displacements $\boldsymbol{u}_s$ have been eliminated from the equation. The reduced TAM can now be defined by premultiplying by the transformation matrix, and the reduced mass matrix becomes

$$\begin{bmatrix} \boldsymbol{I} \\ -\boldsymbol{K}_{\mathrm{ss}}^{-1}\boldsymbol{K}_{\mathrm{sm}} \end{bmatrix}^T \begin{bmatrix} \boldsymbol{M}_{\mathrm{mm}} & \boldsymbol{M}_{\mathrm{ms}} \\ \boldsymbol{M}_{\mathrm{sm}} & \boldsymbol{M}_{\mathrm{ss}} \end{bmatrix} \begin{bmatrix} \boldsymbol{I} \\ -\boldsymbol{K}_{\mathrm{ss}}^{-1}\boldsymbol{K}_{\mathrm{sm}} \end{bmatrix} \approx \boldsymbol{M}_{\mathrm{TAM\_Guyan}} \tag{8}$$

It is important to note that this method gives exact results for static problems. As the solution is derived only from the static stiffness of the system, there will be discrepancies when this is applied to dynamic analyses. As such, the Guyan reduced model will not give an exact match to the eigenvalues and eigenvectors of the full system. This means that, even with an initial full FEM that sufficiently captures the dynamics of the test structure, the reduced model may produce natural frequencies and mode shapes that are different from those in the original FEM and result in noncompliance with correlation checks, such as the COC. The level of imprecision is associated with the neglected inertia of the DOFs not included in the reduction. The method therefore typically becomes less accurate with the increasing natural frequency of considered modes. As the quality of the TAM is heavily dependent on the omitted and selected DOFs, the choice of MPP can significantly affect the accuracy of the final result.

2. System Equivalent Reduction Expansion Process

This work has also considered the SEREP [16] as a potential replacement for the more commonly used Guyan technique for the reduction of spacecraft FEMs, as it was identified previously by

Aglietti et al. [20] as a potentially more suitable method. The main benefit of the SEREP is that it computes a reduced model that matches the eigenvalues and eigenvectors of the full model for the considered DOFs. This approach was originally proposed by Kammer with the development of the modal reduction method [5]. The term SEREP was derived when an adaptation of the original modal reduction was developed by O'Callaghan et al. [16]. The SEREP method presented a significant advantage, as the reduced model gave a true representation of the full model dynamics, therefore providing a potentially more meaningful comparison to the test structure dynamic behavior. It was, however, important to also consider that these benefits might be lessened if the TAM was not robust for dealing with noise and errors in the test and/or FEM results, which could make it more difficult to achieve the required levels of correlation as defined by the COCs [9]. Further investigations into the use of the SEREP for spacecraft FEM reduction, such as those of Aglietti et al. [20] and Sairajan and Aglietti [21], found that the robustness of the TAM to errors was dependent on the number of modes included in the reduction. It was proposed that the robustness might be improved by inclusion of only the target modes in the reduction.

The SEREP method is derived by first defining the displacement of master DOFs as follows:

$$\boldsymbol{u}_m = \boldsymbol{\phi}_m \boldsymbol{\eta} \tag{9}$$

where the target mode shapes, partitioned to the required DOFs, are contained in the modal matrix $\boldsymbol{\phi}_m$, which is multiplied by appropriate modal coordinates contained in the vector $\boldsymbol{\eta}$.

It is then possible to rearrange the preceding equation:

$$\boldsymbol{\eta} = \boldsymbol{\phi}_m^{-1} \boldsymbol{u}_m \tag{10}$$

Often, the number of master DOFs is significantly greater than the number of modes being considered; the following procedure can be performed to obtain the pseudoinverse of the modal matrix:

$$\boldsymbol{\eta} = (\boldsymbol{\phi}_m^T \boldsymbol{\phi}_m)^{-1} \boldsymbol{\phi}_m^T \boldsymbol{u}_m = \boldsymbol{\phi}_m^P \boldsymbol{u}_m \tag{11}$$

where the superscript P represents the pseudoinverse of the reduced modal matrix. It is therefore possible to redefine the full displacement vector $\boldsymbol{u}$ as

$$\boldsymbol{u} = \boldsymbol{\phi}\boldsymbol{\eta} = \boldsymbol{\phi}\boldsymbol{\phi}_m^P \boldsymbol{u}_m \tag{12}$$

If Eq. (12) is substituted into Eq. (4), and the resulting equation is then premultiplied by the transpose of the reduced modal matrix and its pseudoinverse, the result is

$$\boldsymbol{\phi}_M^{P^T} \boldsymbol{\phi}^T \boldsymbol{M} \boldsymbol{\phi} \boldsymbol{\phi}_M^P \ddot{\boldsymbol{u}}_M + \boldsymbol{\phi}_M^{P^T} \boldsymbol{\phi}^T \boldsymbol{K} \boldsymbol{\phi} \boldsymbol{\phi}_M^P \boldsymbol{u}_M = \boldsymbol{\phi}_M^{P^T} \boldsymbol{\phi}^T \boldsymbol{f} \tag{13}$$

With the mode shapes mass normalized, which is commonly performed automatically by FE software, the following holds true:

$$\boldsymbol{\phi}^T \boldsymbol{M} \boldsymbol{\phi} = \boldsymbol{I} \tag{14}$$

Looking back to Eq. (13), it can be seen that the TAM can be represented in the following manner, and is therefore determined from the mode shapes alone:

$$\boldsymbol{M}_{\text{TAM\_SEREP}} = \boldsymbol{\phi}_M^{P^T} \boldsymbol{\phi}_M^P \tag{15}$$

Note that no manipulation of the full FEM mass matrix is needed to obtain $\boldsymbol{M}_{\text{TAM\_SEREP}}$. If required, the reduced stiffness matrix may be derived in the same way. It should be noted that this method of reduction inherently yields modes exactly matching the partitioned full FEM modes.

C. Sensor Placement Optimization Methods

1. *Modal Kinetic Energy Method*

The concept of using energy distribution as a master DOF selection indicator has been in use for decades [45]. This led to the now commonly applied modal KE method [29,46] of sensor placement selection, which is a computationally efficient single calculation method. This method estimates the dynamic contribution of the considered DOFs through use of mass and modal displacement information. This is calculated as follows:

$$\text{KE}_{ik} = \phi_{ik} \sum_j M_{ij} \phi_{jk} \tag{16}$$

where i denotes the DOF index; j is the column of the mass matrix $\boldsymbol{M}$; and k is the target mode number.

This KE calculation may be applied for all of the target modes in order to determine the DOFs associated with maximized KE for the mode under consideration [6]. An appropriate number of DOFs for the final sensor set may then be selected on the basis of the associated KE.

The KE method is therefore a means to improve target mode signal strength. One limitation of this method, however, is that the linear independence of the target modes, which is an important factor to aid in mode identification (and therefore test-analysis correlation), is not considered. Nevertheless, this technique is still commonly used to improve the accuracy in static TAMs. Furthermore, this technique is often used as an initial method to reduce an extremely large sensor set down to a more reasonable starting point to then apply another sensor set optimization method, such as an effective independence-based approach.

2. *Effective Independence Method*

To address the issue of linear independence, as well as signal strength, for the target modes, Kammer [28] developed an iterative method of sensor set selection known as the effective independence method. Other methods previously attempted to address this, but most employed search techniques that required greater computational time and effort [28].

The EFI method takes inspiration from the earlier work of Qureshi et al. [47] by proposing to solve the problem of selecting a sensor set that provides the best numerical conditioning of the Fisher information matrix $\boldsymbol{Q}$. The method is based on the idea that the linear independence between modes is optimized by selecting DOFs to maximize the determinant of the Fisher information matrix. The effective independence matrix can be calculated as follows:

$$\text{EFI}_{ii} = (\phi_a)_i \boldsymbol{Q}^{-1} (\phi_a)_i^T \tag{17}$$

where

$$\boldsymbol{Q} = \boldsymbol{\phi}_a^T \boldsymbol{\phi}_a \tag{18}$$

where $\boldsymbol{\phi}_a$ is the modal matrix, with rows corresponding to the candidate set DOFs and columns representing the modes of interest to be found by modal analysis of the full FEM. The leading diagonal values are then $0 \leq \text{EFI}_{i,i} \leq 1$. The lower the value of the leading diagonal, the less the corresponding DOF contributes to the independence of the mode shapes. Therefore, this method works by eliminating the DOFs with the lowest EFI. The technique is generally applied iteratively, and the ideal case has only one single DOF eliminated in each iteration. This enables the method to account for cases where the elimination of one DOF changes the order of importance of the remaining DOFs. This process is repeated until the desired number of sensors is determined.

This method, and its variations, are commonly applied and recommended in many texts [48–50] as an appropriate method to apply when selecting sensor locations.

III. Example Applications

A. Overview of Investigations Undertaken

The studies presented herein focused on two large, unique, scientific spacecraft (shown in Fig. 1) [51]:

1) The first spacecraft is the ESA/Japan Aerospace Exploration Agency collaboration spacecraft BepiColombo for the exploration of Mercury. It has a stacked configuration comprising two planetary orbiters and a propulsion module. The spacecraft has a mass of 6446 kg, and the FEM consists of approximately 302,065 nodes (1,812,390 DOFs) and 278,030 elements.

2) The second spacecraft is the ESA's Atmospheric Dynamics Mission Aeolus spacecraft for global wind-component-profile observation, which aims to improve weather forecasting. This spacecraft has a mass of 1800 kg, and the FEM consist of approximately 95,980 nodes (575,880 DOFs) and 109,295 elements.

These investigations compare the Guyan and SEREP FEM reduction processes in order to assess their suitability for large spacecraft applications. In addition, a number of different sensor location options have also been examined.

Two sets containing the same number of DOFs as the original test MPP have been assessed:

1) Both Guyan and SEREP have been performed on the original spacecraft test MPP DOFs. The natural frequencies and mode shapes of the reduced models are compared with the original full FEM results (with mode shapes partitioned to the same MPP DOFs) to assess the accuracy of the reduced model at representing the full system dynamics.

2) Alternate sensor locations, with the same number of DOFs as the original MPPs, have been determined through the use of the modal KE approach. With these new sensor locations, the Guyan reduction is again applied to assess whether there is a notable improvement in the orthogonality metric.

Using the initial test MPP DOFs as candidate sets, the effective independence approach is adopted to reduce two new sets half the size of the test MPPs:

1) The first "half-MPP-sized sets" consist of the DOFs that are selected from the MPPs as being the "best-case" half of the MPP for achieving optimal independence between the target modes.

2) The other half-MPP-sized sets consist of the remaining DOFs, which are omitted from the MPPs during the effective independence sensor selection. As such, this set represents a "worst-case" sensor selection to serve as a comparison with the best-case DOFs that are selected from the same original MPPs.

B. Reduction Method Comparisons

To investigate the quality of the TAM generated by the Guyan reduction process and the SEREP, modal analyses have been performed on the BepiColombo and Aeolus FEMs. Here, the "quality assessment" of the reduced models is performed with respect to a consistent full model of each spacecraft. Detailed results are given for BepiColombo, with summaries of the results for both spacecraft also presented herein.

For the purposes of this investigation, the modes of interest have been identified based solely on the modal effective mass of each mode in the translational directions. Modes with a modal effective mass of at least 1% in any translational direction have been selected as target modes, as shown in Table 1 for BepiColombo and Aeolus. The modal effective mass gives an indication to the level of participation of each mode in the loads analysis and is often used to highlight potentially significant modes for correlation [52]. In the case of spacecraft reduced FEMs delivered for launcher-spacecraft CLAs, adequate effective mass capture is deemed "mandatory" for adequate representation of coupled behavior.

Initially, the starting sets of DOFs are those that correspond to the original test MPP of accelerometer positions used during the spacecraft sine-sweep tests. With Guyan reduction, the number of reduced modes identified within the frequency range of interest is dependent on which DOFs are being retained in the reduction; hence, MAC assessments have been performed to determine which reduced mode matched most closely the corresponding selected full target mode (partitioned to the MPP DOFs). It should be noted that, when using MAC to determine the "best match" Guyan reduced mode for each target full (partitioned) mode, it was found that, in some cases, the same reduced mode gave the highest MAC for more than one of the target modes. As a result, some reduced modes have been repeated in order that the best match is given for each target mode in turn. For the SEREP, only the selected target modes have been included in the modal matrix used to derive the reduced modes; thus, only the required reduced modes are present, and no mode matching is required.

Comparisons have been made between the natural frequencies of the full (partitioned) target modes and the reduced modes selected as a best match to these targets based on MAC comparisons. Figure 2 illustrates the reduced model natural frequencies plotted against those calculated from the full FEM for both BepiColombo (left) and Aeolus (right).

The MAC for the matched reduced modes compared with the full partitioned modes of BepiColombo is given in Fig. 3 for both Guyan

Table 1 Modal effective masses of selected target modes

BepiColombo				Aeolus			
	Modal effective mass, %				Modal effective mass, %		
Frequency, Hz	TX	TY	TZ	Frequency, Hz	TX	TY	TZ
12.68	0.66	25.96	0.02	15.96	42.35	0.02	0.00
13.01	25.30	0.73	0.00	16.62	0.02	45.31	0.00
26.50	4.79	0.23	0.00	40.94	0.00	6.89	0.02
27.12	2.40	0.55	0.00	41.30	0.00	3.40	0.02
27.68	1.21	0.00	0.00	48.95	1.50	0.00	0.02
28.43	0.02	8.97	0.07	54.58	2.39	0.14	0.32
32.43	0.11	0.10	1.21	55.63	0.75	0.15	6.76
33.44	0.00	0.12	5.96	56.94	3.65	0.20	0.00
35.82	0.33	1.14	0.08	58.68	0.47	0.58	1.65
37.03	2.91	0.01	2.94	60.00	0.00	0.00	1.84
37.19	0.36	0.19	3.38	61.47	0.00	0.15	1.46
37.55	2.19	0.16	0.05	63.86	0.08	0.00	5.43
37.77	0.50	0.52	13.15	64.35	0.47	0.00	22.90
38.01	0.00	1.13	1.61	64.69	5.45	0.07	2.47
44.07	0.02	0.03	1.32	69.60	0.01	1.04	0.01
44.37	0.16	2.34	0.01	84.64	0.26	0.05	3.65
45.01	0.00	0.00	1.20	85.01	0.02	0.03	1.52
49.10	0.08	0.03	6.95	85.23	0.02	0.01	8.33
49.77	0.00	0.12	1.03	— —	— —	— —	— —
57.01	1.12	0.00	0.02	— —	— —	— —	— —
57.17	2.10	0.00	0.02	— —	— —	— —	— —

Note: TX, TY and TZ refer to the translational X, Y and Z directions.

Fig. 1 BepiColombo (left) and Aeolus (right) during vibration test preparation [51].

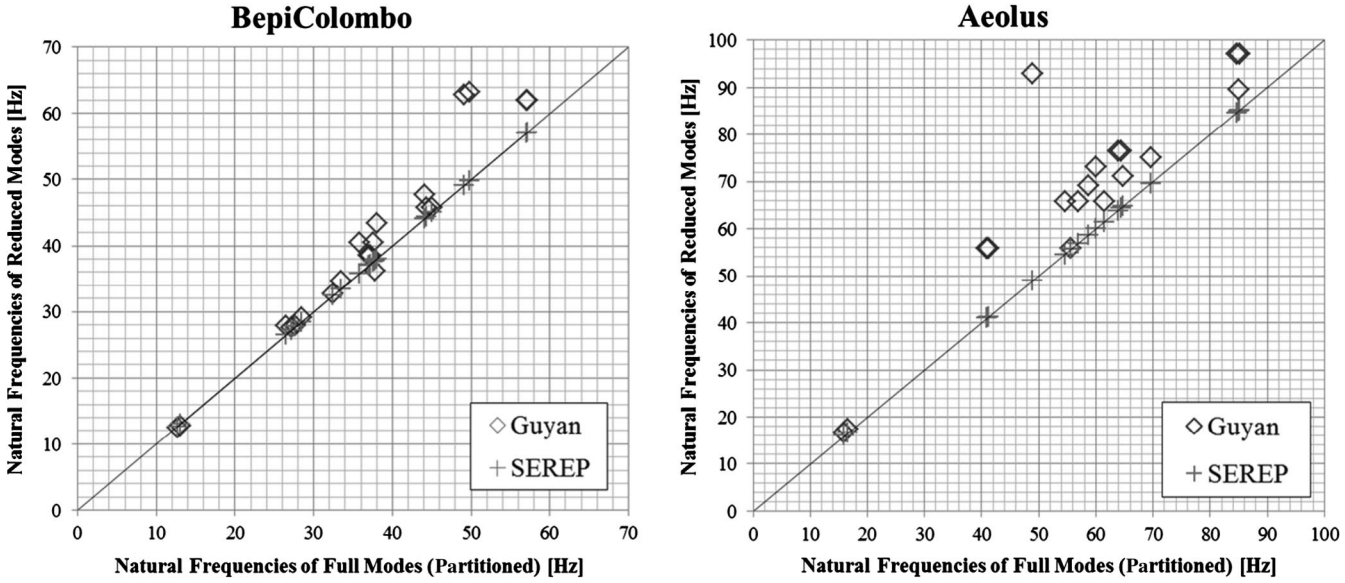

Fig. 2 Natural frequencies (in hertz) for reduced vs full FEMs for BepiColombo (left) and Aeolus (right).

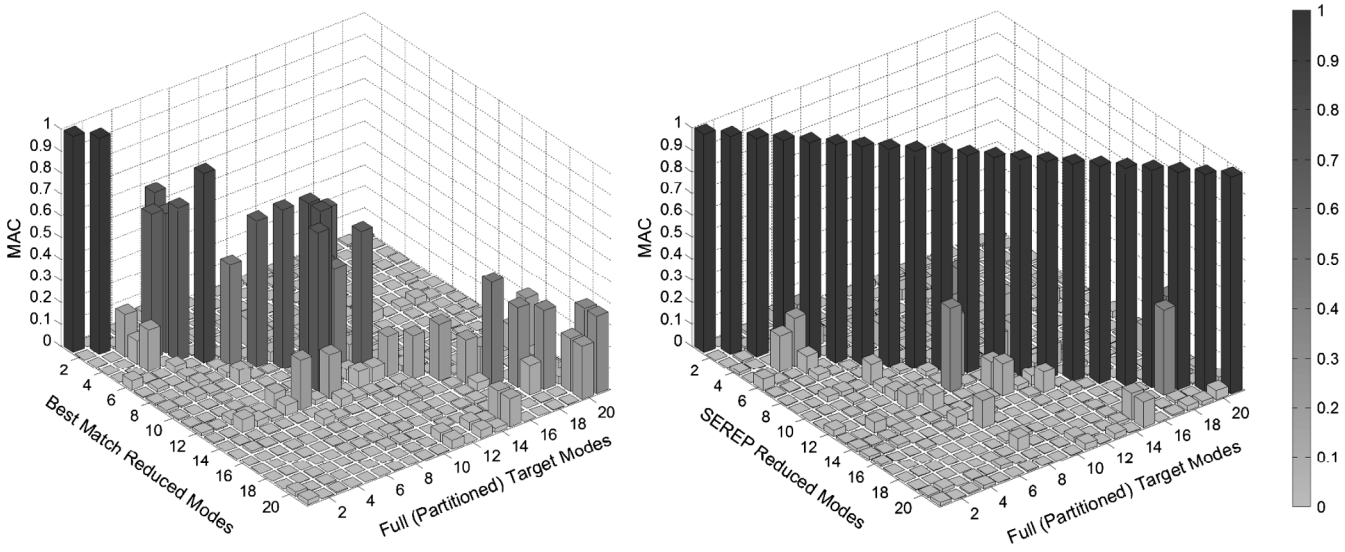

Fig. 3 MAC of reduced and full FEM mode shapes for BepiColombo: Guyan (left), and SEREP (right).

and SEREP. The leading diagonal values provide an indication of how well the "matched" reduced modes represent their targets partitioned from the full FEM results. Figure 4 shows the orthogonality check results obtained using the Guyan and SEREP reduced TAMs. The reduced and full modes are again compared, but now with the reduced mass matrix providing a relative weighting to the DOFs and producing an orthogonality check, in which the offdiagonal values are important indicators of the TAM quality. The full modes are then compared with themselves, using both TAMs to give an indication of the TAM quality.

From Fig. 2, it can be noted that, for the SEREP natural frequencies, the points all lie on the diagonal, indicating a perfect match. For the Guyan reduction, some points deviate from the diagonal, indicating a difference between the reduced and full model results. The natural frequencies of the Guyan reduced models match the targets increasingly poorly as the frequency is increased: for example, going from an almost exact match for the first target mode of BepiColombo at 12.7 Hz to a maximum difference of 28% from the target at 49.8 Hz, with a similar trend found for Aeolus. In general, the static nature of the Guyan reduction, with the neglected inertia of omitted DOFs, will be expected to lead to inaccuracies and overprediction of natural frequencies as frequencies grow higher, but these results serve to highlight the issue in the frequency range of interest.

The MAC (Fig. 3) and COC (Fig. 4a) comparisons of the partitioned full and Guyan reduced modes reveal a poor match in modes other than the first few fundamental modes. This is a notable finding, as it demonstrates the errors introduced as a result of the reduction process, which means that the reduced model is not representative of the full model. Thus, any comparisons between the reduced FEM and test modes are not necessarily indicative of how representative of the real spacecraft the full FEM actually is, even with as many as approximately 400 and 300 test instrumentation DOFs for BepiColombo and Aeolus, respectively.

In contrast, the SEREP method has also been implemented to reduce the FEM to the test-measured DOFs. Here, the reduced model matches the full model results for natural frequencies and mode shapes exactly. This is an inherent aspect of the SEREP process and means that the reduced model is representative of the full model, making comparisons between the reduced model and test results potentially more meaningful.

C. Kinetic Energy Sensor Placement Influence on FEM Reductions

Although the aforementioned results should to some extent be expected, the findings serve to highlight the extent of the lack of accuracy in the Guyan representation of the spacecraft dynamics when the model is reduced to the DOFs used in the original spacecraft sine-sweep test MPP as used in practice. To determine whether these

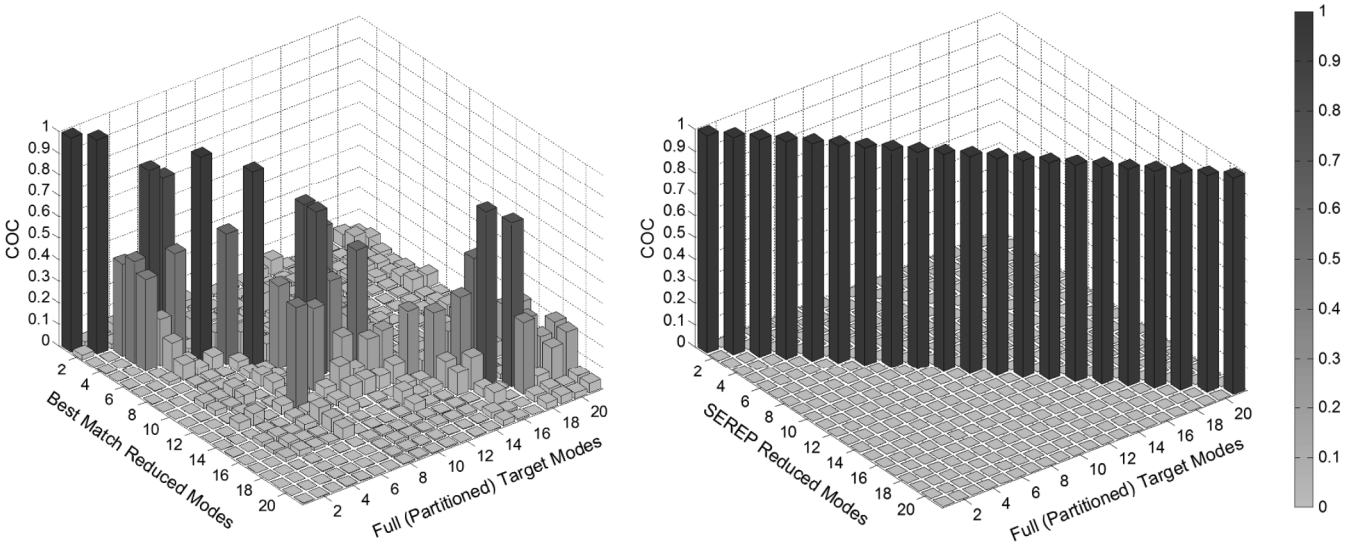

a) Partition of full modes vs reduced modes

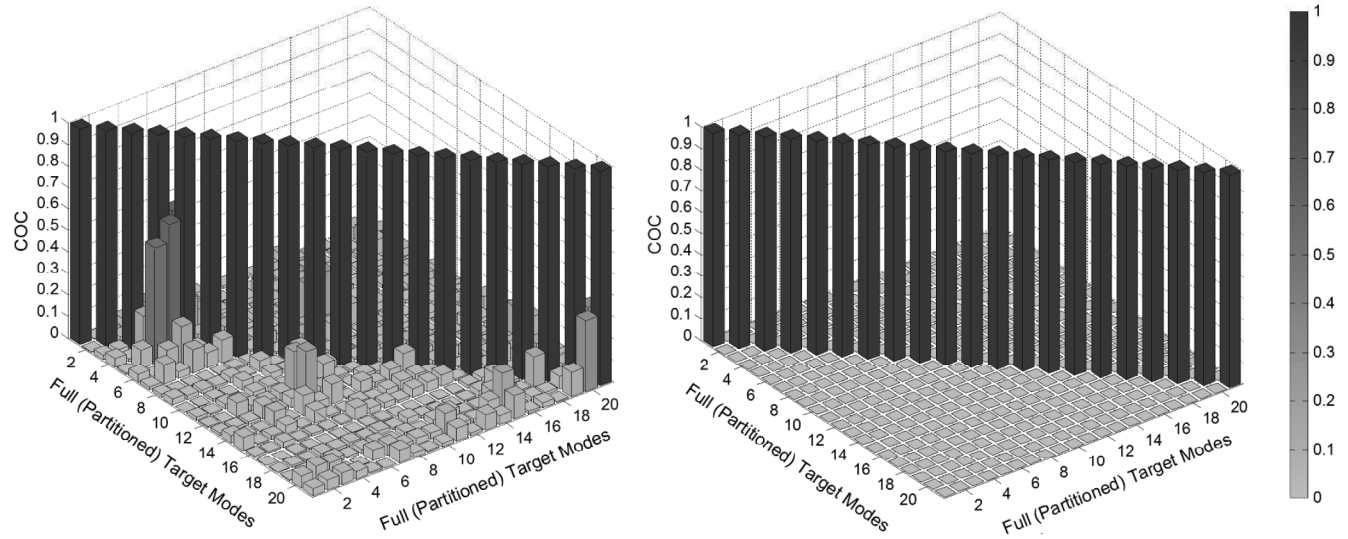

b) Partition of full modes vs partition of full modes

Fig. 4 Cross-orthogonality results for BepiColombo using reduced TAMs: Guyan (left), and SEREP (right).

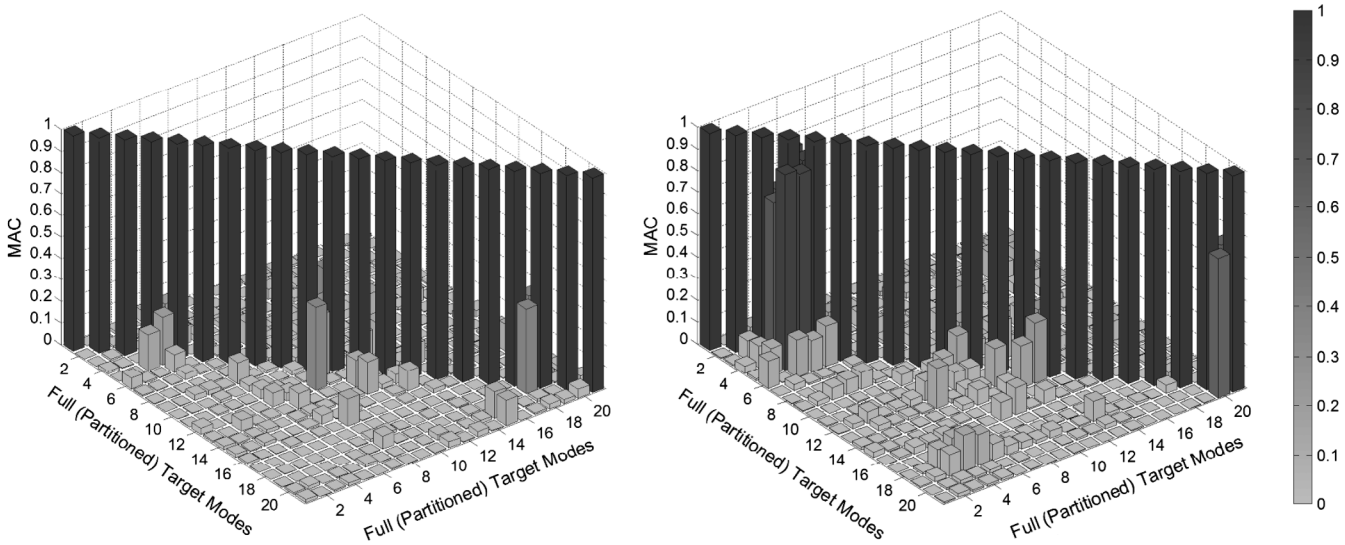

Fig. 5 AutoMAC for BepiColombo target modes: MPP DOFs (left), and KE DOF selection (right).

results are indicative of inherent issues in using Guyan reduction for large spacecraft applications or merely a consequence of poorly selected sensor locations in the original MPP, the use of a different sensor location set, selected on the basis of modal KE, is investigated. To ensure comparisons are meaningful, the number of DOFs in this new KE-based sensor set matches that of the original MPP. For BepiColombo, this means approximately 400 DOFs selected based on kinetic energy and, for Aeolus, a set of approximately 300 DOFs.

AutoMAC is the comparison of the full FEM mode shapes, partitioned to the sensor set DOFs, with themselves through use of the MAC correlation assessment criteria [1]:

$$\text{AutoMAC} = \frac{(\boldsymbol{\phi}_a^T \boldsymbol{\phi}_a)^2}{(\boldsymbol{\phi}_a^T \boldsymbol{\phi}_a) \cdot (\boldsymbol{\phi}_a^T \boldsymbol{\phi}_a)} \tag{19}$$

The leading diagonal will, inherently, yield all unity as each mode perfectly matches itself; it is therefore the offdiagonal terms that are of interest. High offdiagonals indicate a lack of independence between the mode shapes, and therefore imply a potentially poor choice of sensor locations. As such, low offdiagonals reveal a good level of independence between the modes for the selected MPP.

Figure 5 shows three-dimensional (3-D) bar plots of AutoMAC comparisons for the BepiColombo spacecraft target modes (as identified in Table 1). The first image, on the left, shows the AutoMAC for the original MPP; whereas the image on the right is the result of comparisons made using the set with approx. 400 DOFs (the same number of DOFs as the full MPP) selected from the FEM based on the KE method described previously. It can be seen that there are some higher offdiagonal values in the right-hand image compared to those on the left plot. The same deterioration was found for the Aeolus spacecraft when the KE rather than MPP DOF set was applied, as summarized in Table 2. This indicates that the KE method has resulted in a sensor set that makes distinguishing the different modes more difficult than it was for the original MPP. This was to be expected, as the KE method did not optimize based on linear independence between modes but purely on mode signal strength.

The MAC comparisons for BepiColombo of the full model target mode shapes, partitioned to these new KE DOF sets, with the best matched Guyan reduced modes are given in Fig. 6. The original MPP MAC plot is also included again for comparison. The corresponding COCs, performed using the respective Guyan TAMs, are given in Fig. 7. For added clarity, these results are also summarized in Table 2.

The use of modal kinetic energy to determine a new sensor set placement has not resulted in a marked improvement in the accuracy of the Guyan TAM at representing the full FEM. For BepiColombo, the summary in Table 2 reveals no notable improvement in orthogonality check results. There was a slight improvement in the MAC between reduced and corresponding target modes; however,

Table 2 Summary of results for KE selected reduced sensor sets for both spacecraft

		MAC		AutoMAC		Orthogonality check with Guyan TAM			
		Full vs Guyan reduced modes		Full vs full modes		Full vs Guyan reduced modes		Full vs full modes	
		Original MPP	KE selected	Original MPP	KE selected	Original MPP	KE selected	Original MPP	KE selected
BepiColombo									
Diagonals	Maximum	0.9960	0.9956	1.0000	1.0000	0.9989	0.9988	1.0000	1.0000
	Minimum	0.1885	0.0129	1.0000	1.0000	0.0256	0.0621	1.0000	1.0000
	Average	0.5179	0.5791	1.0000	1.0000	0.5422	0.4845	1.0000	1.0000
	% ≥ 0.9	9.52	23.81	100.00	100.00	19.05	9.52	100.00	100.00
Offdiagonals	Maximum	0.7716	0.9922	0.3933	0.9012	0.8173	0.7424	0.6195	0.3849
	Minimum	0.0000	0.0000	0.0000	0.0000	0.0000	0.0000	0.0000	0.0002
	Average	0.0235	0.0445	0.0184	0.0394	0.0425	0.0431	0.0383	0.0292
	% ≤ 0.1	94.76	87.86	94.76	90.00	90.00	90.24	92.86	94.29
Aeolus									
Diagonals	Maximum	1.0000	0.9965	1.0000	1.0000	1.0000	1.0000	1.0000	1.0000
	Minimum	0.1433	0.2529	1.0000	1.0000	0.1741	0.0034	1.0000	1.0000
	Average	0.4607	0.7140	1.0000	1.0000	0.6277	0.5656	1.0000	1.0000
	% ≥ 0.9	11.11	44.44	100.00	100.00	22.22	44.44	100.00	100.00
Offdiagonals	Maximum	0.7559	0.9859	0.9786	0.9696	0.9583	0.7476	0.9875	0.3518
	Minimum	0.0000	0.0000	0.0000	0.0000	0.0000	0.0000	0.0002	0.0001
	Average	0.0378	0.0841	0.0247	0.0677	0.0891	0.0344	0.0682	0.0252
	% ≤ 0.1	88.89	77.78	96.73	77.12	76.14	90.85	81.70	94.12

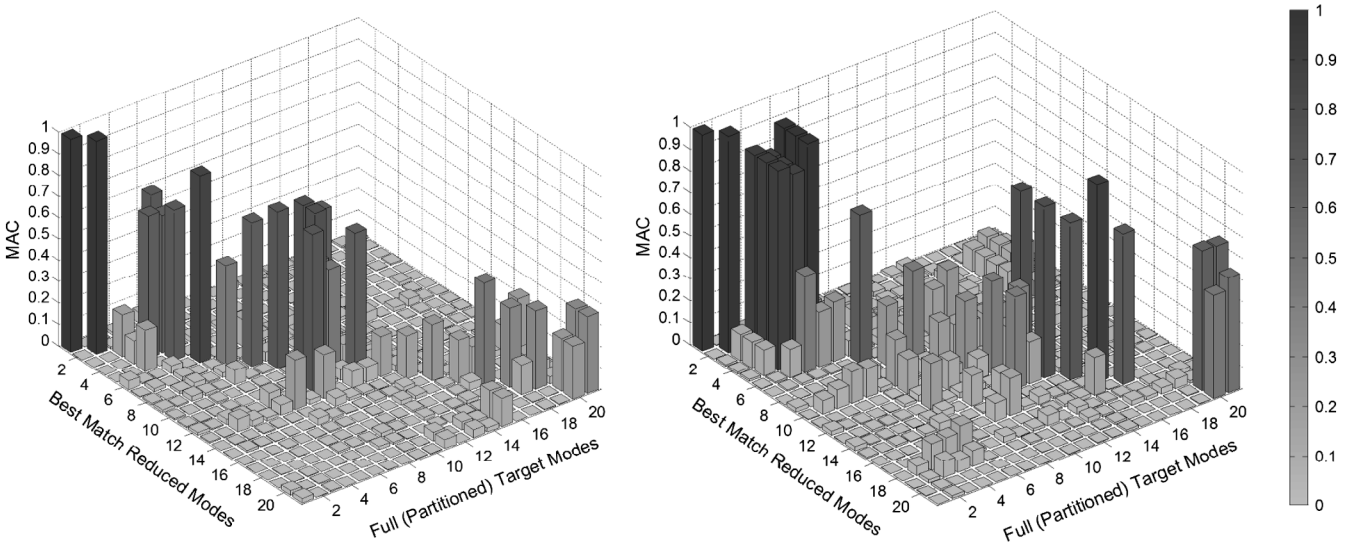

Fig. 6 MAC for BepiColombo full vs Guyan reduced target modes: MPP (left), and KE selected (right).

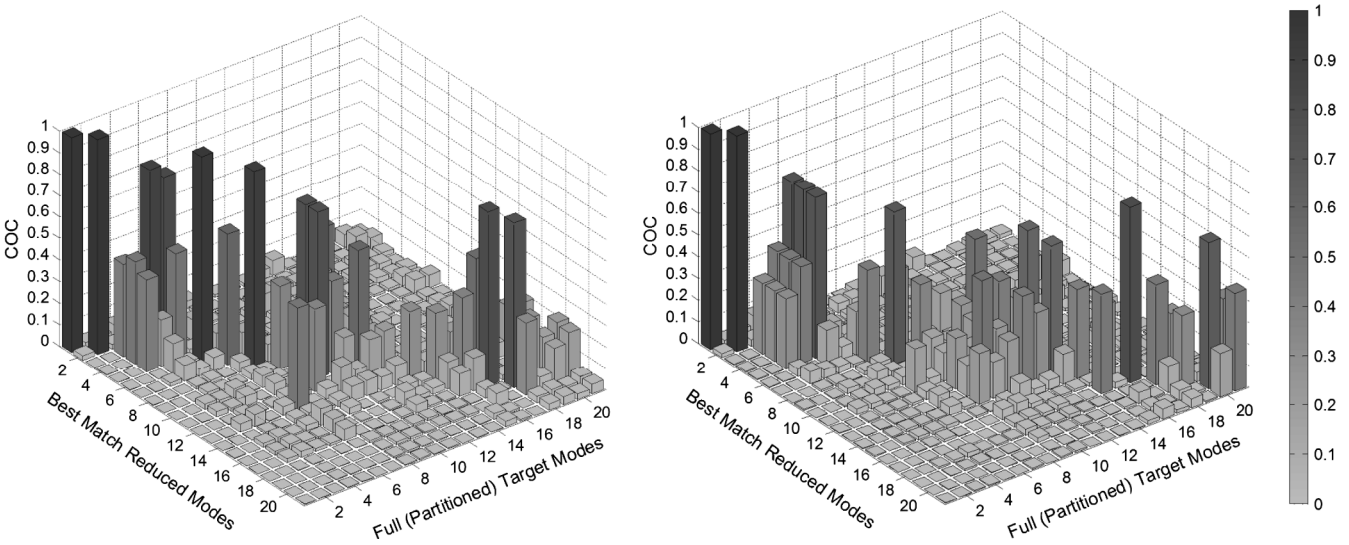

a) Partition of full modes vs guyan reduced modes

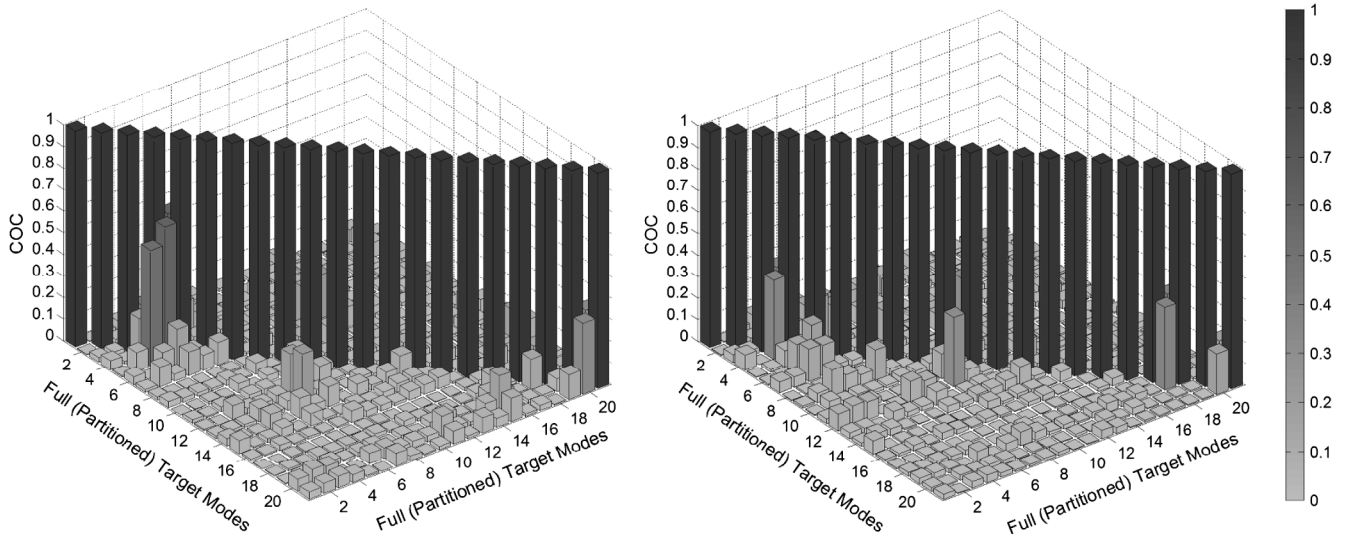

b) Partition of full modes vs partition of full modes

Fig. 7 Orthogonality checks for BepiColombo using Guyan TAM: MPP (left), and KE selected (right).

this was at the cost of less independence between target modes. For Aeolus, the potential benefits of the modal KE approach to sensor placement were more pronounced; with general increases in diagonal terms and decreases in average offdiagonal COC values. Overall, however, it was still observed that, even with this optimized reduced DOF selection, the Guyan reduction did not achieve an accurate representation of the full system for more than a few of the target modes of either spacecraft.

It should be noted that these comparisons have focused on Guyan reduction and the SEREP has not been included. This is the case because the SEREP produces reduced analytical mode shapes and a reduced TAM, which inherently achieved perfect orthogonality with respect to the full FE model modes, regardless of sensor selection. Any SEREP results would only serve to confirm the results in Figs. 3 and 4 and, as such, are omitted here for brevity.

D. Effective Independence Sensor Placement Influence on FEM Reductions

The sensor set locations can have an influence on the quality of TAM generated through model reduction. The influence of sensor set placement for optimum linear independence between modes has also been investigated through the use of the two newly generated sensor sets per spacecraft. For BepiColombo, these sets comprise the best case (approximately 200 DOFs chosen in an EFI method selection based on a candidate set of the original approximately 400 DOFs in the BepiColombo MPP) and an alternative set with the remaining approximately 200 DOFs, which were eliminated in the EFI selection. Likewise for Aeolus, the same approach has been applied to obtain two subsets of approximately 150 DOFs each from the original approximately 300 DOF MPP. To assess the linear independence of target modes, which the EFI method aims to optimize, AutoMAC checks are performed.

Figure 8 shows 3-D bar plots of AutoMAC comparisons for the BepiColombo spacecraft target modes (as identified in Table 1). The original MPP had approximately 400 accelerometers; therefore, the original FEM was reduced to approximately 400 DOFs. Here, this has been reduced further to include only approximately 200 DOFs, selected from the candidate set of original approximately 400 DOFs in the MPP. The first image, on the left, shows a selection derived from the DOFs eliminated by the EFI method; whereas the second image, on the right, is the result of the other DOFs selected using the EFI method. It can be seen that, although there are still some noticeable offdiagonal values in the right-hand image, these are significantly reduced from those on the left plot. The left plot in Fig. 8 shows that the EFI selected DOF set results in a plot closely resembling the AutoMAC for the full MPP, as given previously in Fig. 5, further highlighting the lack of independent information contained in the EFI omitted DOF set. The same improvement is found for the Aeolus spacecraft. This comparison can be useful to check the independence of modes resulting from proposed MPPs, and is therefore a valuable aid in comparing different sensor set location options.

When the Guyan reduction process is applied for the new smaller sensor subsets, even fewer distinct modes are identified by the finite element modal analysis in the frequency range of interest than for the original MPP, as shown in Table 3. It should also be noted that, for both spacecraft, the FEA is able to identify significantly more reduced modes for the EFI selected DOF set than that of the DOFs eliminated by the EFI method.

The MAC comparisons for BepiColombo of the full model target mode shapes, partitioned to these new smaller DOF sets, with the best-matched Guyan reduced modes are given in Fig. 9. The corresponding COCs, performed using the respective Guyan TAMs, are given in Fig. 10. For added clarity, these results are also summarized in Table 4.

The aforementioned results show that, even within the initial BepiColombo MPP sensor set, there is a notable difference in the quality of reduced Guyan model, depending on the selected subset of sensors. For both spacecraft, a higher percentage of the leading diagonal terms are over 0.9 for the EFI selected sensor set, and the offdiagonals are lower, both for the AutoMAC and for the orthogonality checks, compared to the alternative sensor set.

Again, these comparisons have focused only on the quality of Guyan reduced TAMs, as the SEREP produces reduced mode shapes and reduced TAMs, which inherently achieve perfect match and are orthogonal to the partitioned full mode vectors for any reduced DOF set.

E. Comparisons of Test and FEM Using Both Guyan and SEREP Reduction Methods

All of the previous results presented herein have demonstrated the ability of the reduced TAM to represent the full FEM for the purpose of COCs solely through FEM-only comparisons. The same Guyan and SEREP reduced TAMs used in those investigations have also been used to compare the FEM mode shapes (from analyses of the full models, with the modal vectors partitioned to the required DOFs matching the test measured locations) with the mode shapes extracted from the test measured data.

The experimental results used in these comparisons are derived from data captured from MPP accelerometers used during base-shake sine-sweep testing of the considered spacecraft. To obtain modal information from the resulting frequency response function (FRFs), appropriate curve-fitting methods were employed. In this case, the focus is on comparison with FEM normal modes; as such, the normalized test modes are extracted. The modal parameter estimation is of particular importance given the high modal density, particularly with BepiColombo, requiring the implementation of MDOF curve-

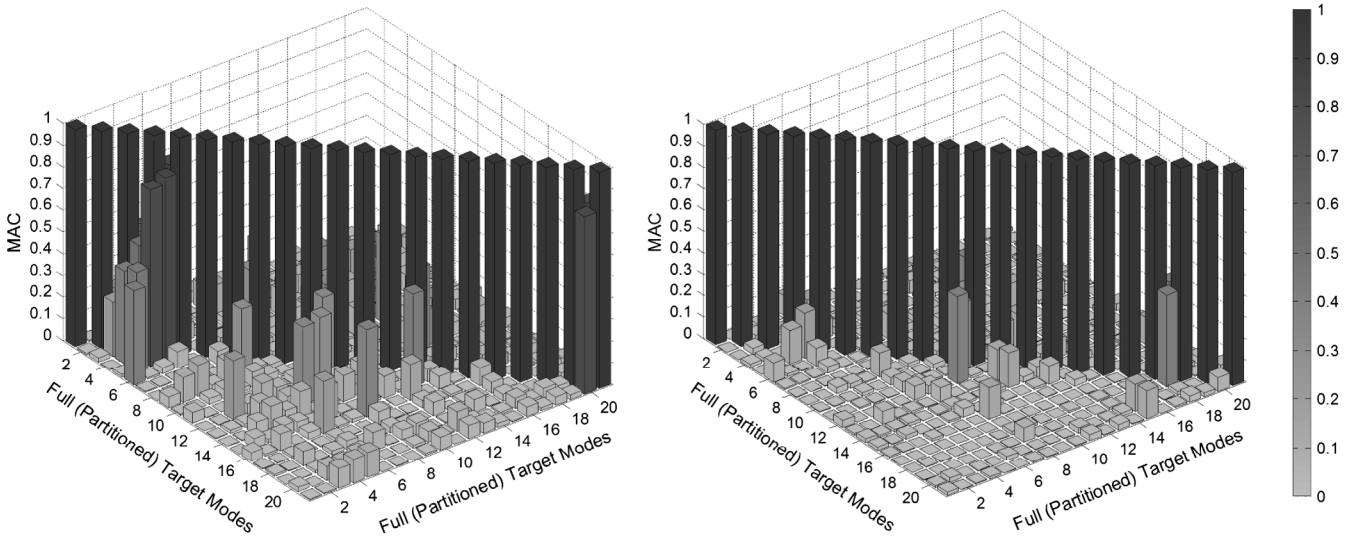

Fig. 8 AutoMAC for BepiColombo target modes: EFI eliminated (left), and EFI selection (right).

Table 3 Number of modes identified in Guyan reduced model in FEA frequency range of interest

		BepiColombo		Aeolus	
Type of run	DOFs used	Number of DOFs (approximate)	No. of modes in FEA (0–100Hz)	Number of DOFs (approximate)	No. of modes in FEA (0–100Hz)
Full run	Full model	100 s of thousands	247	100 s of thousands	197
Guyan reduction	MPP	400	105	300	50
Guyan reduction	KE from full model	400	125	300	88
Guyan reduction	EFI selected from MPP	200	93	150	46
Guyan reduction	EFI omitted from MPP	200	37	150	11

Table 4 Summary of results for EFI selected reduced sensor sets for both spacecraft

		MAC		AutoMAC		Orthogonality check with Guyan TAM			
		Full vs Guyan reduced modes		Full vs full modes		Full vs Guyan reduced modes		Full vs full modes	
		EFI selected	EFI eliminated	EFI selected	EFI eliminated	EFI selected	EFI eliminated	EFI selected	EFI eliminated
BepiColombo									
Diagonals	Maximum	0.9937	0.9918	1.0000	1.0000	0.9981	0.9950	1.0000	1.0000
	Minimum	0.2266	0.1439	1.0000	1.0000	0.0183	0.4225	1.0000	1.0000
	Average	0.5616	0.4550	1.0000	1.0000	0.6011	0.6629	1.0000	1.0000
	% $\geq$ 0.9	14.29	9.52	100.00	100.00	19.05	14.29	100.00	100.00
Offdiagonals	Maximum	0.8739	0.9918	0.4303	0.8434	0.8727	0.9274	0.6068	0.8994
	Minimum	0.0000	0.0000	0.0000	0.0000	0.0000	0.0000	0.0001	0.0006
	Average	0.0246	0.0887	0.0201	0.0597	0.0459	0.1524	0.0472	0.1536
	% $\leq$ 0.1	95.24	80.95	94.76	86.67	90.48	54.29	88.57	46.67
Aeolus									
Diagonals	Maximum	1.0000	0.9993	1.0000	1.0000	1.0000	0.9997	1.0000	1.0000
	Minimum	0.1567	0.2418	1.0000	1.0000	0.1654	0.1842	1.0000	1.0000
	Average	0.4771	0.5793	1.0000	1.0000	0.6299	0.6822	1.0000	1.0000
	% $\geq$ 0.9	11.11	16.67	100.00	100.00	22.22	16.67	100.00	100.00
Offdiagonals	Maximum	0.7620	0.9039	0.9787	0.9875	0.9565	0.9249	0.9871	0.9934
	Minimum	0.0000	0.0000	0.0000	0.0000	0.0000	0.0000	0.0003	0.0002
	Average	0.0372	0.1209	0.0268	0.1090	0.0918	0.2079	0.0713	0.2614
	% $\leq$ 0.1	90.85	69.93	94.12	67.32	74.51	49.35	79.08	28.76

fitting techniques [53]. As such, the extraction of mode shapes used in this study is achieved mainly through the use of the polyreference least-squares complex frequency method [54], which is a popular approach for structures such as those considered herein. Despite the use of one of the most popular current methods, the modal extraction provides only a "best-fit" estimation of the test modes from the available data [50].

As for the purely analytical comparisons presented in the previous section, again, the COCs have been conducted for: 1) the full MPP sets, containing all of the DOFs at which accelerometers captured the response of the structural thermal models; 2) the EFI selected half-sets, which resulted from applying the EFI method to the MPPs in order to identify the "best half" DOFs from the MPP; and 3) the EFI eliminated half-sets, which were those remaining "worst half" DOFs that were not selected when the EFI method was applied to the MPPs.

The modes of interest have again been selected on the basis of modal effective mass, with FEM modes achieving greater than 5% m_{eff} in any translational direction (see Table 1) and the best matching corresponding test modes being included in the test–FEM comparison. The results are summarized in Table 5.

From Table 5, it should be noted that, despite only containing half of the DOFs, the EFI selected DOF set achieves very similar results to

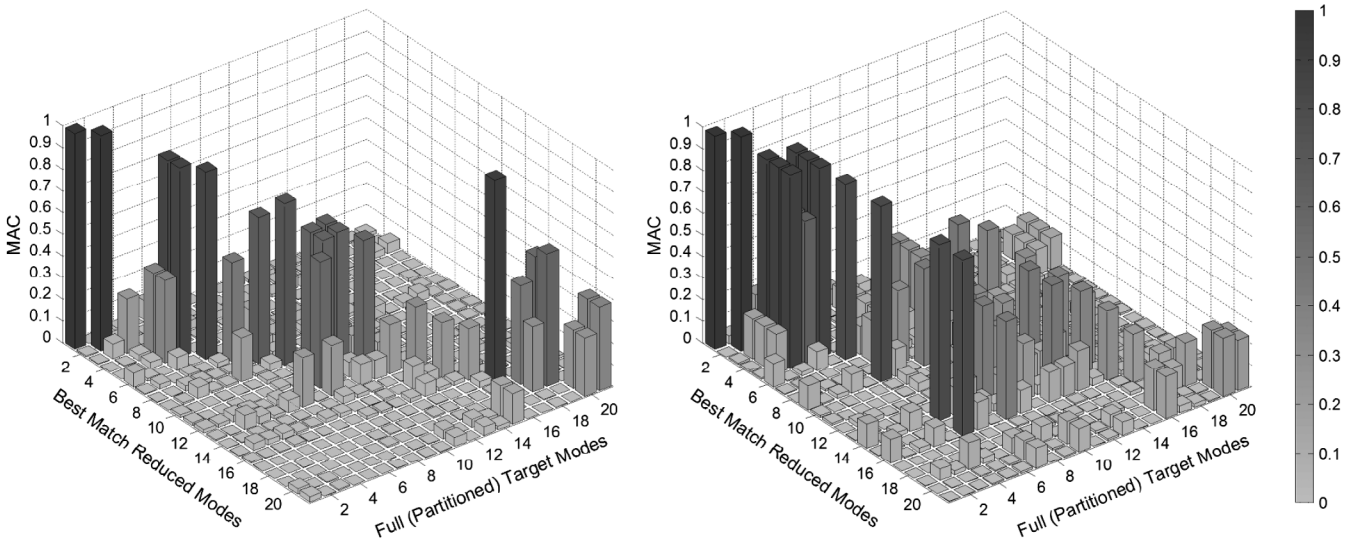

Fig. 9 MAC for BepiColombo full vs Guyan reduced modes: EFI selected (left), and EFI eliminated (right).

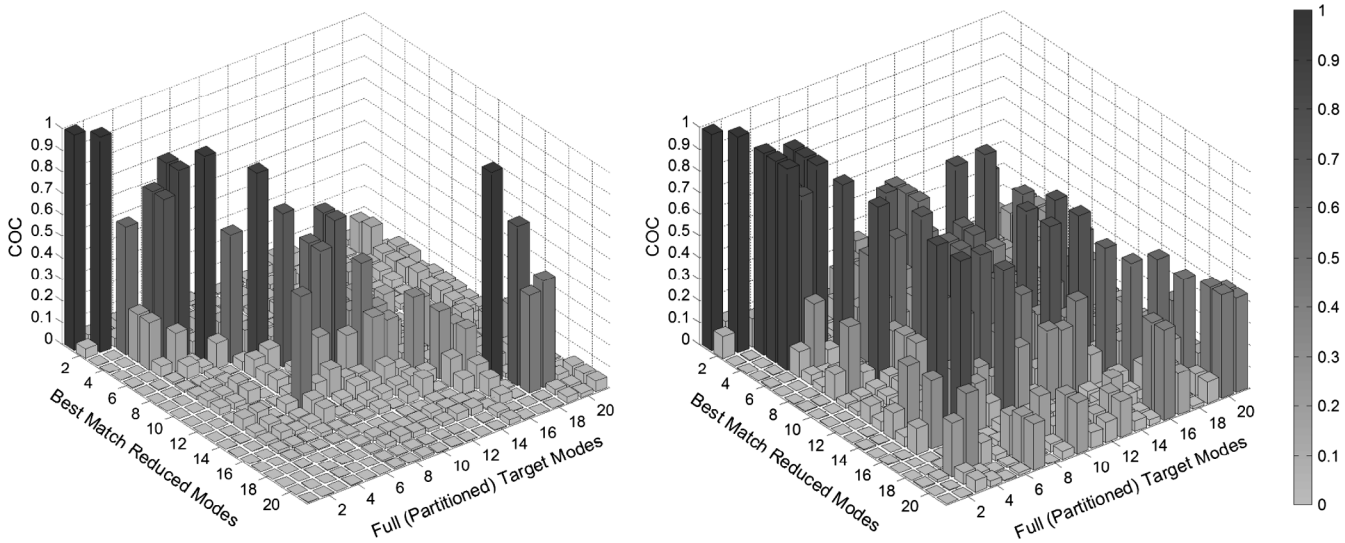

a) Partition of full modes vs guyan reduced modes

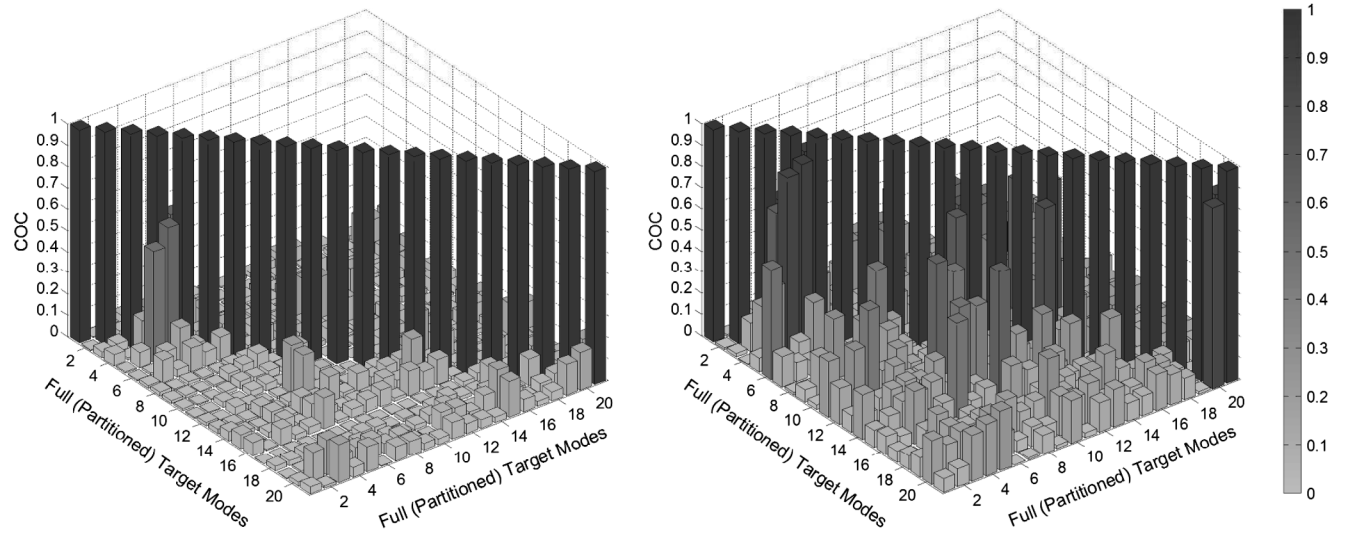

b) Partition of full modes vs partition of full modes

Fig. 10 Orthogonality checks for BepiColombo using Guyan TAM: EFI selected (left), and EFI eliminated (right).

the full MPP set. This is most clearly evident for Aeolus, but it is also demonstrated in the average, maximum, and minimum diagonal values for BepiColombo.

Both the full MPP and EFI selected sets show the SEREP TAM achieves markedly higher leading diagonal values than the orthogonality checks conducted with Guyan TAM, but at the cost of the offdiagonal values also being slightly higher for the SEREP than Guyan. For the EFI eliminated sets, these trends are reversed, with higher cross-orthogonality values in Guyan (both diagonal and offdiagonal) and lower diagonal values for the SEREP. It should, however, be noted that the Guyan reduced TAMs used to generate the EFI eliminated results are those demonstrated previously (see Table 4) as giving the poorest representation of the full FEM.

It should be reiterated that, in practice, the ultimate purpose of these COCs is the correlation and update of the FEM for use in subsequent analyses to ensure the structure is able to withstand events that cannot be fully replicated in the test environment. As such, it is vital that the reduced models are giving a true representation of the full FEM in order that genuine differences between test and FEM are highlighted for further investigation, as well as being robust enough not to be adversely influenced by inevitable minor inconsistencies in test and FEM responses.

During correlation activities, it was found that many of the required FEM updates, identified through examination of many correlation criteria including COCs such as those presented herein, related to issues with initial modeling assumptions [55]. One of the more common issues in both spacecraft FEMs was the internal boundary conditions, particularly in relation to internal joints represented through the use of rigid-body RBE2 elements. The common application of "RBE2 spiders" to provide connections was found, in certain cases, to result in the introduction of "point flexibilities" at the connecting nodes/grid points of the FEM structure. In BepiColombo, for example, the result was that the eigenfrequencies of some regions of the structure were lower than was seen in the test. Although, in itself, this could be considered a relatively minor issue, this localised frequency shift meant that some local modes, which in the test occurred at different frequencies, were seen to arise at the same frequency as each other in the FEM. As a result, in certain cases, different regions of the FEM were found to interact together and demonstrate local modal coupling which was not representative of the behavior observed during the test. Additionally, the assumptions surrounding the addition of nonstructural mass also required a FEM update in order to address similar unrepresentative coupling of local modes. In the case of BepiColombo, the manner of using a "smeared" nonstructural mass to represent the multilayer insulation on a panel resulted in unrepresentative coupling with the vibration modes a pressurant tank, which had been modeled with lumped mass and had not provided the correct moment of inertia. Identifying issues such as these with the FE modeling was essential in order to have confidence that the FEM was reliable for further analyses. This served to underline

Table 5 Summary of results comparing test and finite element analyses for both spacecraft: full FEM modes[a] vs test modes

		Orthogonality check with SEREP TAM			Orthogonality check with Guyan TAM		
		Full MPP	EFI selected	EFI eliminated	Full MPP	EFI selected	EFI eliminated
BepiColombo							
Diagonals	Maximum	0.9821	0.9811	0.9115	0.9123	0.9639	0.9817
	Minimum	0.4396	0.4047	0.0084	0.0333	0.0231	0.0510
	Average	0.8000	0.7769	0.4854	0.6132	0.6094	0.6883
	% $\geq$ 0.9	50.00	50.00	16.67	33.33	16.67	33.33
Offdiagonals	Maximum	0.1962	0.2353	0.1426	0.1882	0.2147	0.4365
	Minimum	0.0002	0.0027	0.0015	0.0010	0.0026	0.0009
	Average	0.0757	0.0947	0.0466	0.0405	0.0585	0.1139
	% $\leq$ 0.1	73.33	53.33	93.33	90.00	83.33	60.00
Aeolus							
Diagonals	Maximum	0.9918	0.9911	0.6386	0.9687	0.9724	0.9906
	Minimum	0.3283	0.3549	0.0163	0.0677	0.0241	0.0842
	Average	0.6561	0.6583	0.3341	0.5677	0.5608	0.6424
	% $\geq$ 0.9	37.50	37.50	0.00	25.00	25.00	37.50
Offdiagonals	Maximum	0.7385	0.7315	0.5503	0.6767	0.6609	0.9033
	Minimum	0.0029	0.0006	0.0018	0.0002	0.0016	0.0124
	Average	0.1256	0.1287	0.1643	0.0931	0.0917	0.2484
	% $\leq$ 0.1	58.93	60.71	48.21	75.00	73.21	37.50

[a]Partitioned to required degrees of freedeom.

how crucial it was to apply correlation techniques that were meaningful and understood rather than focusing on meeting arbitrary criteria through means that might not be representative, such as was demonstrated for the use of Guyan reduction on applications such as those considered in this work.

IV. Conclusions

In this work, the traditional Guyan reduction method was compared with a modal SEREP approach for FEMs of two spacecraft: BepiColombo and Aeolus. For the original test MPP DOFs, the Guyan reduced models matched poorly with the full models, only achieving MAC in excess of 0.9 for approximately 10% of the selected target modes for both spacecraft. When a kinetic energy approach was adopted to obtain a new sensor set (with the same number of DOFs as the original MPPs), this percentage increased to over 23% for BepiColombo and 44% for Aeolus. As such, it was shown that a modal KE-based sensor set selection had the potential to slightly improve the quality of results from Guyan reduction. It was, however, important to note that there was still a significant difference in the results between full and Guyan reduced models. This discrepancy between full and Guyan reduced models might undermine the use of Guyan TAMs in COCs intended to assess the level of correlation between the test structure dynamics and those of the full FEM.

To further study the influence of sensor placement on reduced model quality, the original MPPs for both spacecraft were treated as candidate sets, and smaller sets (half the size) were selected by effective independence: an optimized set (selected from the MPP based on independence), and a worst-case set, containing the remaining half of the MPP (omitted during optimization for displaying poor effective independence). The AutoMAC checks showed significantly lower offdiagonals with the selected DOFs than with those eliminated in the effective independence selection. The Guyan reduction-based orthogonality check offdiagonal values were also markedly lower for the effective independence selected set than for the worst-case omitted set. Although the improvement was slightly less pronounced for the leading diagonal values, it was nevertheless evident that effective independence had the potential to be a useful tool in refining sensor sets.

The SEREP method is theoretically advantageous in that, regardless of the sensor placement, it inherently produces an accurate TAM, in which the natural frequencies and mode shapes match exactly to those of the full FEM and there is perfect orthogonality with the reduced mass matrix. The potential practical benefits of the SEREP are confirmed through the cross-orthogonality comparisons of FEM results with corresponding test-derived mode shapes. For both of the structures considered, it is evident that, when good sensor placement is employed, the SEREP produces consistently higher leading diagonal cross-orthogonality values than the Guyan TAMs.

Acknowledgment

The authors wish to thank Airbus Defence and Space United Kingdom for providing the spacecraft finite element models and funding for this study.

References

[1] Allemang, R. J., and Brown, D. L., "A Correlation Coefficient for Modal Vector Analysis," *Proceedings of the 1st International Modal Analysis Conference*, Soc. for Experimental Mechanics (SEM), Inc., Bethel, CT, 1982, pp. 110–116.

[2] Wijker, J. J., *Mechanical Vibrations in Spacecraft Design*, Springer, New York, 2004, p. 15, 343–367.

[3] Allemang, R. J., "The Modal Assurance Criterion–Twenty Years of Use and Abuse," *Journal of Sound and Vibration*, Vol. 37, No. 8, 2003, pp. 14–23.

[4] Avitabile, P., "Model Reduction and Model Expansion and Their Applications–Part 1 Theory," *IMAC-XXIII: Conference & Exposition on Structural Dynamics*, Soc. for Experimental Mechanics (SEM), Inc., Bethel, CT, 2005.

[5] Kammer, D. C., "Test-Analysis Model Development Using an Exact Modal Reduction," *International Journal of Analytical and Experimental Modal Analysis*, Vol. 2, No. 4, 1987, pp. 174–179.

[6] Bergman, E. J., Allen, M. S., Kammer, D. C., and Mayes, R. L., "Probabilistic Investigation of Sensitivities of Advanced Test-Analysis Model Correlation Methods," *Journal of Sound and Vibration*, Vol. 329, No. 13, 2010, pp. 2516–2531. doi:10.1016/j.jsv.2010.01.009

[7] Koutsovasilis, P., and Beitelschmidt, M., "Comparison of Model Reduction Techniques for Large Mechanical Systems," *Multibody System Dynamics*, Vol. 20, No. 2, 2008, pp. 111–128. doi:10.1007/s11044-008-9116-4

[8] Chung, Y.-T., and Simonian, S. S., "Assessments of Model Correlation Using Dynamic Reduction and Static Reduction," SAE Technical Paper 881527, Warrendale, PA, 1988. doi:10.4271/881527

[9] Freed, A. M., and Flanigan, C. C., "A Comparison of Test-Analysis Model Reduction Methods (Mass and Stiffness Matrix Reduction of Finite Element Model of Large Aerospace Structures)," *8th International Modal Analysis Conference (IMAC)*, Soc. for Experimental Mechanics (SEM), Inc., Bethel, CT, 1990, pp. 1344–1351.

[10] Flanigan, C. C., "Model Reduction Using Guyan IRS and Dynamic Methods," *IMAC XVI — 16th International Modal Analysis Conference*, SDRC Operations, Inc., Soc. for Experimental Mechanics (SEM), Inc., Bethel, CT, 1998, pp. 172–176.

[11] Avitabile, P., Pechinsky, F., and O'Callahan, J., "Study of Modal Vector Correlation Using Various Techniques for Model Reduction," *Proceedings of the International Modal Analysis Conference (IMAC)*, Soc. for Experimental Mechanics (SEM), Inc., Bethel, CT, 1992, pp. 572–572.

[12] Friswell, M. I., Garvey, S. D., and Penny, E. T. J., "Model Reduction Using Dynamic and Iterated IRS Techniques," *Journal of Sound and Vibration*, Vol. 186, No. 2, 1995, pp. 311–323. doi:10.1006/jsvi.1995.0451

[13] Guyan, R. G., "Reduction of Stiffness and Mass Matrices," *AIAA Journal*, Vol. 3, No. 2, Sept. 1964, pp. 380–380.

[14] O'Callahan, J. C., "A Procedure for an Improved Reduced System (IRS) Model," *Proceedings of the 7th International Modal Analysis Conference (IMAC)*, Soc. for Experimental Mechanics (SEM), Inc., Bethel, CT, 1989, pp. 17–21.

[15] Paz, M., "Dynamic Condensation," *AIAA Journal*, Vol. 22, No. 5, 1984, pp. 724–727. doi:10.2514/3.48498

[16] O'Callahan, J., Avitabile, P., and Riemer, R., "System Equivalent Reduction Expansion Process (SEREP)," *Proceedings of the 7th International Modal Analysis Conference*, 1989, pp. 29–37.

[17] Kammer, D., "A Hybrid Approach to Test-Analysis-Model Development for Large Space Structures," *Journal of Vibration and Acoustics*, Vol. 113, No. 3, 1991, pp. 325–332. doi:10.1115/1.2930188

[18] Bampton, M. C., Craig, J., and Roy, R., "Coupling of Substructures for Dynamic Analyses," *AIAA Journal*, Vol. 6, No. 7, 1968, pp. 1313–1319. doi:10.2514/3.4741

[19] "MSC Nastran," Software Package, MSC Software Corp., Newport Beach, CA, 2013.

[20] Aglietti, G. S., Walker, S. J. I., and Kiley, A., "On the Use of SEREP for Satellite FEM Validation," *Engineering Computations*, Vol. 29, No. 2, 2012, pp. 580–595. doi:10.1108/02644401211246292

[21] Sairajan, K. K., and Aglietti, G. S., "Robustness of System Equivalent Reduction Expansion Process on Spacecraft Structure Model Validation," *AIAA Journal*, Vol. 50, No. 11, 2012, pp. 2376–2388. doi:10.2514/1.J051476

[22] Kientzy, D., Richardson, M., and Blakely, K., "Using Finite Element Data to Set Up Modal Tests," *Sound and Vibration Magazine*, Vol. 23, No. 6, 1989, pp. 16–23.

[23] Jarvis, B., "Enhancements to Modal Testing Using Finite Elements," *9th Conference International Modal Analysis Conference (IMAC)*, Soc. for Experimental Mechanics (SEM), Inc., Bethel, CT, 1991, pp. 402–408.

[24] Udwadia, F., "Methodology for Optimum Sensor Locations for Parameter Identification in Dynamic Systems," *Journal of Engineering Mechanics*, Vol. 120, No. 2, 1994, pp. 368–390. doi:10.1061/(ASCE)0733-9399(1994)120:2(368)

[25] Langenhove, T. V., and Brughmans, M., "Using MSC/Nastran and LMS/PRETEST to Find an Optimal Sensor Placement for Modal Identification and Correlation of Aerospace Structures," LMS International, Leuven, Belgium, 1999.

[26] Papadimitrio, C., "Optimal Sensor Placement Methodology for Parametric Identification of Structural Systems," *Journal of Sound and Vibration*, Vol. 278, Nos. 4–5, 2004, pp. 923–947. doi:10.1016/j.jsv.2003.10.063

[27] Kammer, D. C., "Sensor Set Expansion for Modal Vibration Testing," *Mechanical Systems and Signal Processing*, Vol. 19, No. 4, 2005, pp. 700–713. doi:10.1016/j.ymssp.2004.06.003

[28] Kammer, D. C., "Sensor Placement for On-Orbit Modal Identification and Correlation of Large Space Structures," *Journal of Guidance, Control, and Dynamics*, Vol. 14, No. 2, 1991, pp. 251–259. doi:10.2514/3.20635

[29] Salama, M., Rose, T., and Garba, J., "Optimal Placement of Excitations and Sensors for Verification of Large Dynamical Systems," *Proceedings of the 28th Structures, Structural Dynamics, and Materials Conference*, AIAA, Reston, VA, 1987, pp. 6–8. doi:10.2514/6.1987-782

[30] Kammer, D. C., and Tinker, M. L., "Optimal Placement of Triaxial Accelerometers for Modal Vibration Tests," *Mechanical Systems and Signal Processing*, Vol. 18, No. 1, 2004, pp. 29–41. doi:10.1016/S0888-3270(03)00017-7

[31] Helfrick, M. N., Niezrecki, C., Avitabile, P., and Schmidt, T., "3-D Digital Image Correlation Methods for Full-Field Vibration Measurement," *Mechanical Systems and Signal Processing*, Vol. 25, No. 3, 2011, pp. 917–927. doi:10.1016/j.ymssp.2010.08.013

[32] Chu, T., Ranson, W., and Sutton, M., "Applications of Digital-Image-Correlation Techniques to Experimental Mechanics," *Experimental Mechanics*, Vol. 25, No. 3, 1985, pp. 232–244. doi:10.1007/BF02325092

[33] Siebert, T., Wood, R., and Splitthof, K., "High Speed Image Correlation for Vibration Analysis," *Journal of Physics: Conference Series*, Vol. 181, No. 1, 2009, Paper 012064.

[34] Stanbridge, A. B., and Ewins, D. J., "Modal Testing Using a Scanning Laser Doppler Vibrometer," *Mechanical Systems and Signal Processing*, Vol. 13, No. 2, 1999, pp. 255–270. doi:10.1006/mssp.1998.1209

[35] Stanbridge, A. B., Martarelli, M., and Ewins, D. J., "Measuring Area Vibration Mode Shapes with a Continuous-Scan LDV," *Measurement*, Vol. 35, No. 2, 2004, pp. 181–189. doi:10.1016/j.measurement.2003.07.005

[36] Warren, C., Niezrecki, C., Avitabile, P., and Pingle, P., "Comparison of FRF Measurements and Mode Shapes Determined Using Optically Image Based, Laser, and Accelerometer Measurements," *Mechanical Systems and Signal Processing*, Vol. 25, No. 6, 2011, pp. 2191–2202. doi:10.1016/j.ymssp.2011.01.018

[37] Wang, W., Mottershead, J. E., and Mares, C., "Vibration Mode Shape Recognition Using Image Processing," *Journal of Sound and Vibration*, Vol. 326, Nos. 3–5, 2009, pp. 909–938. doi:10.1016/j.jsv.2009.05.024

[38] Wang, W., Mottershead, J. E., Ihle, A., Siebert, T., and Reinhard Schubach, H., "Finite Element Model Updating from Full-Field Vibration Measurement Using Digital Image Correlation," *Journal of Sound and Vibration*, Vol. 330, No. 8, 2011, pp. 1599–1620. doi:10.1016/j.jsv.2010.10.036

[39] Wang, D., DiazDelaO, F. A., Wang, W., Lin, X., Patterson, E. A., and Mottershead, J. E., "Uncertainty Quantification in DIC with Kriging Regression," *Optics and Lasers in Engineering*, Vol. 78, March 2016, pp. 182–195. doi:10.1016/j.optlaseng.2015.09.006

[40] Li, Y. Y., Cheng, L., Yam, L. H., and Wong, W. O., "Identification of Damage Locations for Plate-Like Structures Using Damage Sensitive Indices: Strain Modal Approach," *Computers and Structures*, Vol. 80, No. 25, 2002, pp. 1881–1894. doi:10.1016/S0045-7949(02)00209-2

[41] Kang, L.-H., Kim, D.-K., and Han, J.-H., "Estimation of Dynamic Structural Displacements Using Fiber Bragg Grating Strain Sensors," *Journal of Sound and Vibration*, Vol. 305, No. 3, 2007, pp. 534–542. doi:10.1016/j.jsv.2007.04.037

[42] dos Santos, F. L. M., Peeters, B., Lau, J., Desmet, W., and Góes, L. C. S., "An Overview of Experimental Strain-Based Modal Analysis Methods," *Proceedings of the International Conference on Noise and Vibration Engineering (ISMA)*, Leuven, Belgium, 2014, pp. 2453–2468.

[43] *ECSS-E-ST-32-11 Modal Survey Assessment*, European Cooperation for Space Standardization, ESA-ESTEC, Noordwijk, The Netherlands, 2008, p. 78.

[44] "Load Analyses of Spacecraft and Payloads," NASA STD 5002, 1996, p. 20.

[45] Popplewell, N., Bertels, A., and Arya, B., "A Critical Appraisal of the Elimination Technique," *Journal of Sound and Vibration*, Vol. 31, No. 2, 1973, pp. 213–233. doi:10.1016/S0022-460X(73)80376-1

[46] Parker, G. R., Rose, T. L., and Brown, J. J., "Kinetic Energy Calculation as an Aid to Instrumentation Location in Modal Testing," *MSC World Users Conference Proceedings*, Vol. II, Paper No. 47, March 1990.

[47] Qureshi, Z., Ng, T., and Goodwin, G., "Optimum Experimental Design for Identification of Distributed Parameter Systems," *International Journal of Control*, Vol. 31, No. 1, 1980, pp. 21–29. doi:10.1080/00207178008961025

[48] Ewins, D., *Modal Testing: Theory, Practice and Application*, 2nd ed., Research Studies Press, Ltd., Baldock, Hertfordshire, England, U.K., 2000, pp. 511–513.

[49] Friswell, M., and Mottershead, J. E., *Finite Element Model Updating in Structural Dynamics*, Vol. 38, Solid Mechanics and Its Applications, Springer, Dordrecht, The Netherlands, 1995, pp. 71–75. doi:10.1007/978-94-015-8508-8

[50] Heylen, W., Lammens, S., and Sas, P., *Modal Analysis Theory and Testing*: Katholieke Univ. Leuven, Faculty of Engineering, Dept. of Mechanical Engineering, Division of Production Engineering, Machine Design and Automation, Leuven, Belgium, 2013, pp. 27–29, Part A, Chap. 6.

[51] Space in Images, http://www.esa.int/spaceinimages/Images, ESA [retrieved 16 Feb. 2015].

[52] Chung, Y. T., and Sernaker, M. L., "Assessment Target Mode Selection Criteria Payload Modal Survey," *IMAC XII — 12th International Modal*

Analysis Conference, McDonnell Douglas Aerospace (USA), Soc. for Experimental Mechanics (SEM), Inc., Bethel, CT, 1994.

[53] Mercer, J. F., Aglietti, G. S., and Kiley, A. M., "Modal and Frequency Domain Based Techniques for Finite Element Model Correlation," *CompDYN 2015 Conference Proceedings e-Book*, Vol. 1, edited by Papadrakakis, M., Papadopoulos, V., and Plevris, V., 2015, pp. 191–208.

[54] Guillaume, P., Verboven, P., Vanlanduit, S., Van Der Auweraer, H., and Peeters, B., "A Poly-Reference Implementation of the Least-Squares Complex Frequency-Domain Estimator," *Proceedings of International Modal Analysis Conference (IMAC)*, Soc. for Experimental Mechanics (SEM), Inc., Bethel, CT, 2003, pp. 183–192.

[55] Mercer, J. F., Kiley, A. M., and Aglietti, G. S., "BepiColombo: Sine Test FEM Correlation Experiences," *Proceedings of the ISMA2014 Conference*, ISMA, KU Leuven, Leuven, Belgium, 2014, pp. 835–850.

C. Bisagni
Associate Editor